Research Article

polymers advanced technologies

Received: 9 September 2009, Revised: 6 December 2009, Accepted: 6 January 2010, Published online in Wiley Online Library: 24 February 2010

(wileyonlinelibrary.com) DOI: 10.1002/pat.1672

Effect of PEO-PPO-PEO copolymer on the mechanical and thermal properties and morphological behavior of biodegradable poly (L-lactic acid) (PLLA) and poly (butylene succinate-co-L-lactate) (PBSL) blends

V. Vilay[a,b], M. Mariatti[a]*, Zulkifli Ahmad[a], K. Pasomsouk[b] and Mitsugu Todo[c]

A blend of two biodegradable and semi-crystalline polymers, poly (L-lactic acid) (PLLA; 70 wt%) and poly (butylene succinate-co-L-lactate) (PBSL; 30 wt%), was prepared in the presence of various polyethylene oxide-polypropylene oxide-polyethylene oxide (PEO-PPO-PEO) triblock copolymer contents (0.5, 1, 2 wt%). Mechanical, thermal properties, and Fourier transform infrared (FTIR) analysis of the blends were investigated. It was found that the addition of copolymer to PLLA/PBSL improved the fracture toughness of the blends as shown by mode I fracture energies. It was supported by morphological analysis where the brittle deformation behavior of PLLA changed to ductile deformation with the presence of elongated fibril structure in the blend with copolymer system. The glass transition temperature (T_g), melting temperature (T_m) of PLLA, and PBSL shift-closed together indicated that some compatibility exists in the blends. In short, PEO-PPO-PEO could be used as compatibilizer to improve the toughness and compatibility of the PLLA/PBSL blends. Copyright © 2010 John Wiley & Sons, Ltd.

Keywords: polymer blend; poly (L-lactic acid) (PLLA); copolymer; poly (butylene succinate-co-L-lactate) (PBSL)

INTRODUCTION

Poly (L-lactic acid) (PLLA) is an optically active, biodegradable, and biocompatible semi-crystalline polyester that is used for various applications.[1–3] PLLA has strength and modulus comparable to those of commercially available engineering polymers. However, PLLA exhibits brittle fracture behavior, especially under impact loading conditions, and therefore, the toughening of PLLA becomes one of the most important issues in the field of biopolymer engineering.[4] Blending with a ductile polymer is known as an effective way to improve the toughness of a base brittle polymer. The common ductile biodegradable polymers used in such PLLA blending are poly (ε-caprolactone) (PCL),[5–8] poly (butylene succinate) (PBS),[9–11] poly (butylene succinate-co-L-lactate) (PBSL)[9,11,12] and poly (butylene succinate-co-e-caprolactone) (PBSC),[13] and poly (ethylene succinate) (PES).[14] As known, polymer–polymer blending yields new materials with improved properties and better features than those of the blended polymers.[15,16] In most cases, blends are formed by immiscible components and for some thermodynamic reasons, they do not mix with each other; rather, after blending, they form phase-separated microstructures or morphologies.[5–13,16]

The improvement of miscibility between the polymer components and the enhancement of blend performance is denominated by compatibilization. This compatibilization can be achieved by chemical methods and also by using ionizing radiation. Polyethylene Oxide (PEO) was found to be miscible to most ethylene-based polymers, for example with PBS and PES, to the extent of forming interpenetrating spherulite structure.[17–20] Similarly, partial miscibility was observed in blending polymethyl methacrylate with poly (propylene oxide-b-ethylene oxide) which was attributed to entropic factor and hydrogen bonding with the hydroxyl end group.[21] In addition, it was found that incorporation of copolymer of ethylene oxide and propylene

* *Correspondence to: M. Mariatti, School of Materials and Mineral Resources Engineering, Universiti Sains Malaysia, 14300 Nibong Tebal, Pulau Pinang, Malaysia.*
E-mail: mariatti@eng.usm.my

a *V. Vilay, M. Mariatti, Z. Ahmad*
School of Materials and Mineral Resources Engineering, Universiti Sains Malaysia, 14300 Nibong Tebal, Pulau Pinang, Malaysia

b *V. Vilay, K. Pasomsouk*
Department of Mechanical Engineering, Faculty of Engineering, National University of Laos, P.O. Box 3166, Vientiane, Laos

c *M. Todo*
Research Institute for Applied Mechanics, Kyushu University, Kasuga, Fukuoka, Japan

Contract/grant sponsor: AUN/SEED-Net and JICA; contract/grant number: 6050131.

polymers advanced technologies

oxide surfactant (co-PEO/PPO) can effectively improve the immiscibility in PLLA/PCL or poly-dl-lactic acid (PDLLA) blends and as a result, improve their mechanical properties.[8] Based on these studies, the triblock copolymer PEO-PPO-PEO was used as a compatibilizer in improving miscibility between PLLA and PBSL. To the best of our knowledge, there is no scientific literature describing the effect of PEO-PPO-PEO on the properties of PLLA/PBSL blends. Its content in PLLA/PBSL blend was varied at 0.5, 1, and 2 wt%. The effect of this copolymer content on PLLA/PBSL blends was likewise investigated. Various characterization methods, such as mode I fracture, dynamic mechanical analysis (DMA), differential scanning calorimetry (DSC) analysis, thermogravimetry analysis (TGA), Fourier transform infrared (FTIR), and morphological studies, have been carried out to compare the characteristics of the blends.

EXPERIMENTAL

Materials

PLLA pellets of medical grade (Lacty®#5000, $M_w = 1.45 \times 10^5$, $M_n = 0.75 \times 10^5$, PD = 1.93) were supplied by Toyota Motor Co. Ltd. PLLA is a thermal plastic material derived from lactic acid, with a glass transition temperature (T_g) of around 57°C and a melting point temperature (T_m) of around 180°C. PBSL pellets of type GS Pla® AZ-type (lactate unit *ca.* 3%, $M_w = 1.47 \times 10^5$, $M_n = 0.6 \times 10^5$, PD = 2.5 and DP = 479.8) were supplied by Mitsubishi Chemical Corporation. The T_g and T_m of PBSL are 33 and 113.6°C, respectively. The PEO-PPO-PEO triblock copolymer liquid was supplied by Advanced Polymer Materials Inc. ($M_n = 3500$, $M_w = 3700$). Figure 1 shows the chemical structures of (a) PLLA, (b) PBSL, and (c) PEO-PPO-PEO triblock copolymer.[16,22]

Blend preparation

The virgin PLLA and PLLA polymer blends were prepared by melt-mixing in a two-roll-mill heater machine at a temperature of 190°C for 10 min. The blend ratios of PLLA/PBSL were fixed at 70/30 wt% and the PEO-PPO-PEO triblock copolymer content was varied from 0.5, 1, and 2 wt%. After the compounding process, the samples were then compression molded at the temperature of 190°C for 7 min, followed by the cooling process. Table 1 shows the sample compositions and sample coding used in the present study.

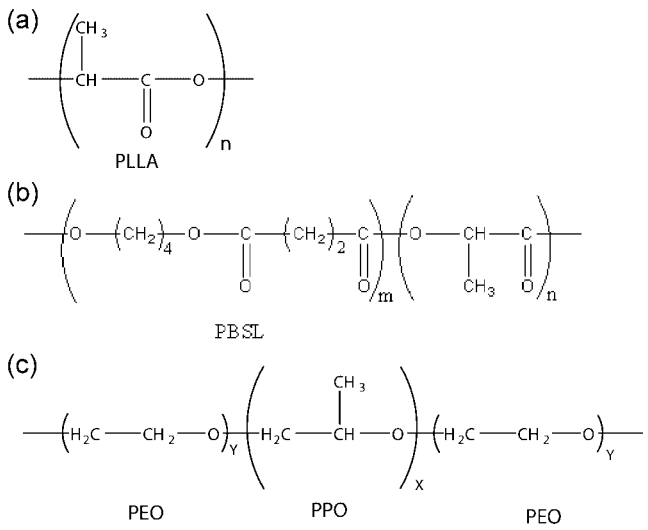

Figure 1. The chemical structures of (a) PLLA, (b) PBSL, and (c) triblock copolymer.

Table 1. Sample designation and composition of materials

Sample code	Composition	Weight % (wt%)
PLLA	PLLA	100
PBSL	PBSL	100
PASL	PLLA/PBSL	70/30
PASL 0.5	PLLA/PBSL/Copolymer	70/30/0.5
PASL 1	PLLA/PBSL/Copolymer	70/30/1
PASL 2	PLLA/PBSL/Copolymer	70/30/2

Measurements

The FTIR measurement was carried out using Perkin Elmer Spectrum One spectrometer with a resolution of 2 cm^{-1} for four scans over a wavenumber range of 4000–400 cm^{-1}. The film samples were obtained by casting polymer solution on the KRS-5 disk. The solvent (chloroform) was evaporated at room temperature for at least 5 min before recording the infra-red (IR) spectra.

Three-point flexural tests were performed using a servo-hydraulic testing machine according to ASTM-D790. Flexural testing was performed at a cross-head speed of 1 mm/min and the span length was fixed at 40 mm of span configuration. At least five specimens were tested to obtain the average and standard deviation (SD).

The mode I fracture tests of the single-edge-notch bend (SENB) specimens were performed at 1 mm/min of loading-rate using a servo-hydraulic testing machine. The J-integral at crack initiation, J_{in}, was evaluated using the following formula:

$$J_{in} = \frac{\eta U_{in}}{B(W-a)} \quad (1)$$

where U_{in} is the critical energy at crack initiation that was defined as the point where the stiffness of the specimen starts to decrease rapidly; B and W are the specimen thickness and width, respectively; a is the initial crack length; η is the geometrical correction factor; and $\eta = 2$ is the standard SENB specimen.

The average mode I fracture energy, J_f, is defined by the following formula:

$$J_f = \frac{U_f}{B(W-a)} \quad (2)$$

where U_f is the total fracture energy that is dissipated by the complete fracture of the specimen. Thus, J_f is recognized as the average energy per unit area of fracture surface. At least five specimens were tested to obtain the average and SD.

The dynamic mechanical properties of the samples were measured using a Mettler Toledo Model DMA 861 conducted in a dual cantilever mode at a frequency of 1 Hz. The temperature was increased at 5°C/min over the range of −100 to 150°C. The

dimensions of the samples were approximately 50 mm in length, 12 mm in width, and 3 mm in thickness. TGA was conducted by a Perkin Elmer Pyrist 6 TGA analyzer. The temperature range of 30–650°C at a heating rate of 10 °C/min under nitrogen atmosphere was used. Perkin Elmer DSC-7 was used to determine the T_m, T_c, and T_g of the virgin and blend samples. Approximately 8–10 mg of the samples were weighted and put into an aluminum pan with a cover. The samples were then scanned from −70 to 210°C at a scan rate of 10 °C/min, held for 1 min at 210°C, followed by the cooling process from 210 to −70°C at 20 °C/min. The second cycle was carried out at the same heating rate to determine the thermal property of the samples. The intrinsic degree of crystallinity X_{cPLLA} (%) was determined based on Equation (3).

$$X_{cPLLA}(\%) = \frac{(\Delta H_c - \Delta H_m) \times 100}{93 \times X_{PLLA}} \quad (3)$$

where ΔH_c and ΔH_m are the enthalpies of crystallization and melting of PLLA, respectively, and the constant of 93 J/g is the fusion enthalpy of PLLA.[23] X_{PLLA} is the weight fraction of PLLA.

Field emission scanning electron microscopy (FE-SEM) of the cryo-fracture surfaces was performed using a Leo Supra 35VP to characterize the phase morphology of the PLLA blends. The fracture surfaces were obtained by immersing the materials in liquid nitrogen (N_2) for about 30 min. These fracture surfaces were then coated by sputtering with gold. The microstructure of the virgin PLLA and PBSL and PLLA blends were also characterized by observing the fracture surfaces of SEBN specimens under liquid nitrogen environment using FE-SEM.

RESULTS AND DISCUSSION

Mode I fracture property

Figure 2(i) shows load–displacement curves obtained from the mode I fracture tests. Clearly, the addition of copolymer in the PLLA/PBSL blends shows an improvement in the mechanical behavior, compared to those of the PLLA/PBSL blend and the virgin PLLA and PBSL. A sudden drop of the load appearing in the PLLA suggests that the crack growth behavior is brittle. On the other hand, the PBSL shows a slow reduction of load, which corresponds to ductile deformation. There is no significant difference in the curve pattern for the PLLA/PBSL blend with the addition of copolymer with respect to the virgin PLLA. However, it is clearly seen that the maximum load increases and the slope of the curve becomes gentle after the load reaches its maximum. This indicates that the addition of copolymer changes the morphology and mechanical properties of the blends. It is therefore expected that the dissipated energy in the PLLA/PBSL/PEO-PPO-PEO blends during crack growth is much larger than those in the PLLA/PBSL blend and the virgin PLLA. It is also noted that, with the addition of copolymer, the initial slope of the PLLA/PBSL curve (Fig. 2(ii)) is slightly lower than that of the PLLA; this indicates the reduction of stiffness of the specimen.

Figure 3 shows the fractured energy of virgin polymers and the blends. It is seen that the virgin PBSL shows higher J_{in}, corresponding to a ductile polymer. On other hand, the presence of copolymer in PLLA/PBSL blends improved both J_{in} and J_f of the blends, compared to those of the PLLA/PBSL and the virgin PLLA and PBSL. The improvement of J_f is more significant than J_{in}, corresponding to the drastic change of crack

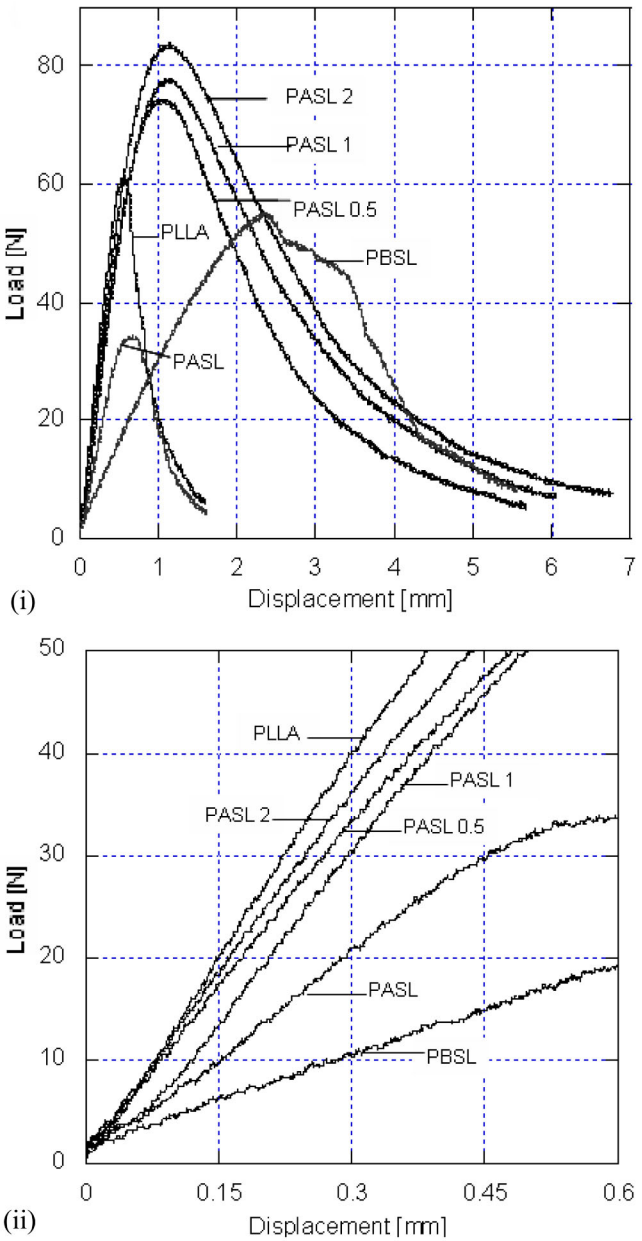

Figure 2. (i) Load–displacement curves of virgin PLLA and PBSL and its blends with and with out PEO-PPO-PEO triblock copolymer; (ii) The initial slope of the load-displacement curves.

growth behavior from brittle to ductile manner as shown in Fig. 2. However, both J_{in} and J_f show similar trends with the increase in copolymer contents, where both fracture energies increase with a higher amount of copolymer added to the blend systems.

The FE-SEM micrographs of the mode I fracture surfaces at the crack propagation region are shown in Fig. 4. The fracture surface of PLLA is flat and smooth corresponding to the lower dissipated energy during crack propagation as shown in Fig. 4(i), whereas the PBSL shows ductile deformation behavior with elongated fibril structures. On the other hand, the PASL sample exhibits very rough surface and two-phase morphology and it can be seen clearly in Fig. 4(iii). This morphology consists of the dispersed phases of PBSL in the continuous PLLA phase.

polymers advanced technologies

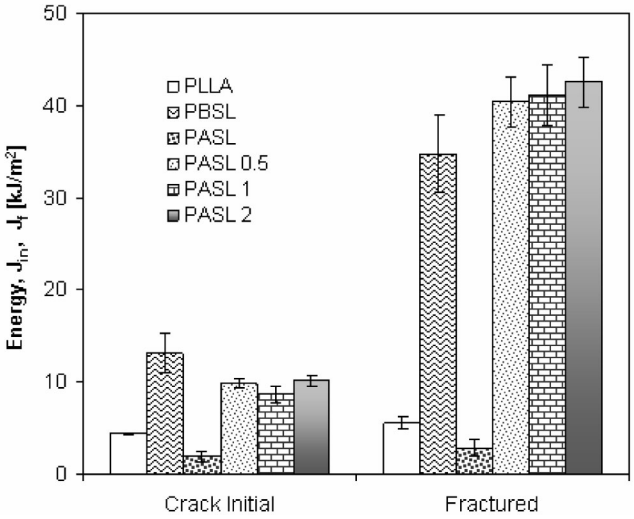

Figure 3. Effect fracture energy of triblock copolymer addition on PLLA/PBSL blend.

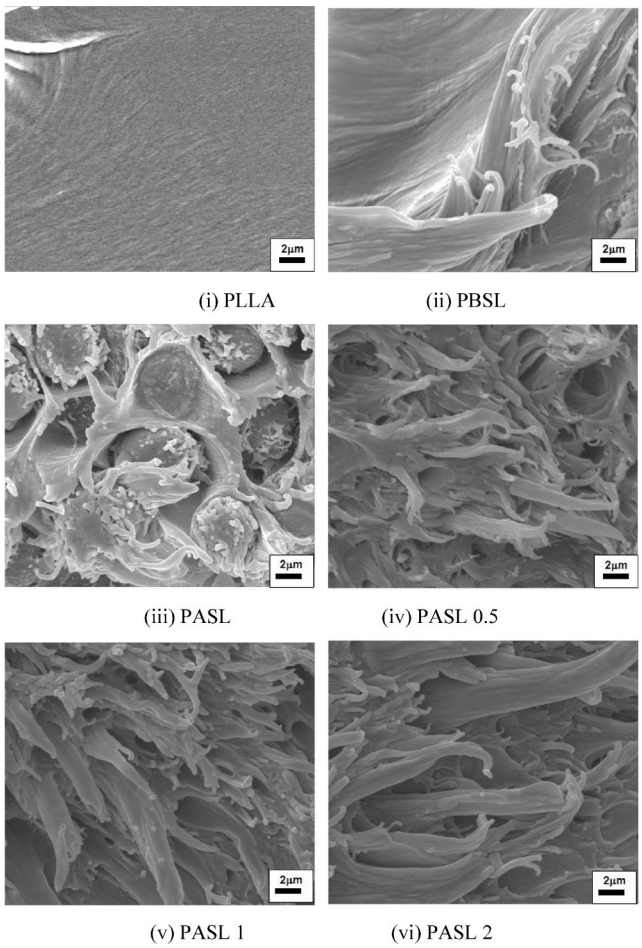

Figure 4. FE-SEM micrographs of mode I fractured surfaces in crack propagation region.

Table 2. Bending properties of virgin PLLA and PBSL and their blends (with and without addition of copolymer)

Samples	Strength (MPa)	Modulus (GPa)	Displacement at break (mm)
PLLA	99.62 ± 7.1	3.99 ± 0.35	4.9 ± 0.51
PBSL	38.50 ± 2.6	1.27 ± 0.13	11.27 ± 0.5
PASL	79.10 ± 3.8	3.41 ± 0.2	4.3 ± 0.6
PASL 0.5	83.50 ± 1.1	3.29 ± 0.4	10.33 ± 0.4
PASL 1	83.27 ± 1.34	3.60 ± 0.17	10.54 ± 0.6
PASL 2	85.60 ± 8.85	3.67 ± 0.28	10.65 ± 0.5

Apparently, voids exist in the vicinity of the dispersed phase and these initiate localized microdamages in this region. The dispersed phase disappeared in the fracture surface of the blends with increased copolymer contents. The morphology turns to fibril structures, and the fibril structures become elongated with the addition of a higher amount of copolymer, that is, a longer fibril structure is observed in PASL 2 (Fig. 4(vi)). Based on the elongated fibril as shown by the micrographs in Fig. 4, it is apparent that the J_f of the blends filled with copolymer are larger than those of the PASL and virgin PLLA.

Bending property

Bending properties, such as bending modulus, strength, and displacement of virgin polymers and blends, are shown in Table 2. Figure 5 exhibits the load versus displacement of bending testing for the virgin PLLA and PBSL and PLLA/PBSL blends, with and without copolymer. Comparable bending displacement and increase in strength and modulus of the PLLA/PBSL blends is

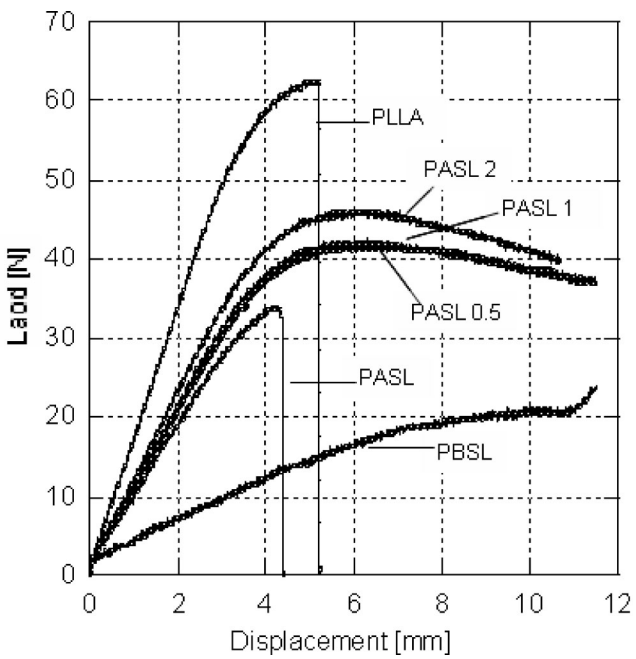

Figure 5. Bending load–displacement curves of virgin PLLA and PBSL and its blends with and without PEO-PPO-PEO triblock copolymer.

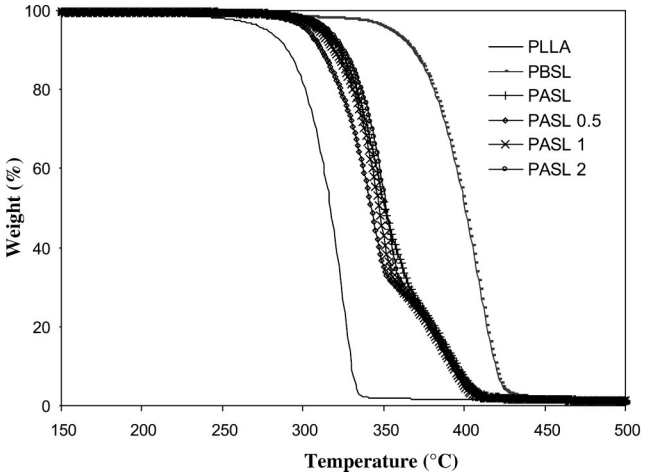

Figure 6. TGA thermograms of virgin PLLA and PLLA/PBSL blend with different copolymer contents.

observed with the addition of copolymer in comparison with PBSL. Furthermore, the incorporation of copolymer in PLLA/PBSL blends increases the toughness (indirectly shown by the area under the load–displacement curves). These trends resemble those of mode I fracture properties in Fig. 3. According to the previous works,[24,25] PLLA can be greatly toughened by copolymerization. As indicated by morphological and DSC studies, some miscibility is occurring in the PLLA/PBSL blend with the addition of copolymer in the PLLA/PBSL blends.

TGA measurements

Figure 6 shows the TGA curves of the virgin PLLA and PBSL and PLLA/PBSL blends with and without different copolymer contents, and all the data are summarized in Table 3. The thermal onset degradation temperature of PLLA and PBSL showed a simple decomposition profile in a single step, while the blends are characterized by two degradation steps. The initial degradation temperature ($T_{5\%}$) and final degradation temperature ($T_{90\%}$) were measured at 5 and 90% of weight loss, respectively. The PBSL shows the highest thermal stability and the PLLA exhibits the lowest thermal stability at both initial and final degradation temperatures. It is noted that the incorporation of PEO-PPO-PEO copolymer in the PLLA/PBSL blend does not significantly increase the initial thermal stability of the PLLA/PBSL blend.

Table 3. The initial degradation temperature ($T_{5\%}$) and final degradation temperature ($T_{90\%}$) of virgin PLLA and PBSL and the PLLA/PBSL blends, with and without the addition of copolymer

Materials	$T_{5\%}$ (°C)	$T_{90\%}$ (°C)
PLLA	277	330
PBSL	354	419
PASL	311	396
PASL 0.5	303	394
PASL 1	310	392
PASL 2	315	392

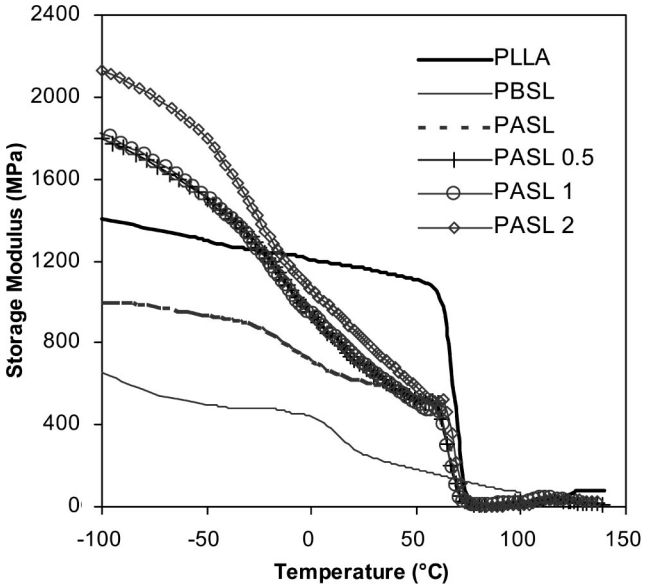

Figure 7. The storage modulus (E′) of virgin PLLA and PLLA/PBSL blends with and without triblock copolymer.

Dynamic mechanical analysis (DMA)

Figure 7 shows plots of the dynamic storage modulus (E′) as a function of temperature for the virgin PLLA and PBSL and PLLA/PBSL blends, with and without the copolymer. For the virgin PLLA, the E′ fell abruptly at approximately 62°C, representing the onset of the glass transition (T_g). An increase in the E′ after T_g in most of the blends, shown in Fig. 7, is indicative of a cold crystallization of amorphous PLLA.[26] For PBSL, the E′ transition seems to occur over a broader range of temperature. The results are in accordance with the previous works.[9] For the PLLA/PBSL blend, the E′ decreased when PBSL (30 wt%) filled to PLLA (70 wt%); the decreasing trend occurred at approximately 57°C. With the addition of copolymer, the E′ at −100°C to −30°C of PLLA/PBSL blends increased and it is apparent that the E′ at this region increased with the increase in triblock copolymer contents. As expected, since these polymer blends exhibit two T_gs, the E′ fell in a broader range and fell abruptly at approximately 60°C.

Differential scanning calorimetry (DSC) and morphology

Figure 8 shows the DSC curves for second heating thermograms of virgin polymers and PLLA/PBSL blends, with and without the addition of copolymer. The degree of crystallinity of PLLA, PBSL, and their blends are summarized in Table 4. In the virgin PLLA thermogram (Fig. 8), the heat jump corresponding to the T_g of PLLA occurs at about 61°C, followed by a cold crystallization exothermic at about 100°C and a melting peak at about 174°C. The DSC of virgin PBSL reveals that its T_m occurred at about 111°C. However, the phase transition or T_g of virgin PBSL and PASL component cannot be seen clearly from the curves. With the addition of copolymer, there are three exothermic peaks observed in the thermograms, which refer to typical cold crystallization of PLLA at 90°C, before the melting point of PLLA and small peak at −20°C. The peak at −20°C might be due to the phase transition or T_g of PBSL (in as much as the T_g of PBSL is −33°C, as reported by the manufacturer). The peculiar exothermic event before the melting point has been observed

polymers advanced technologies

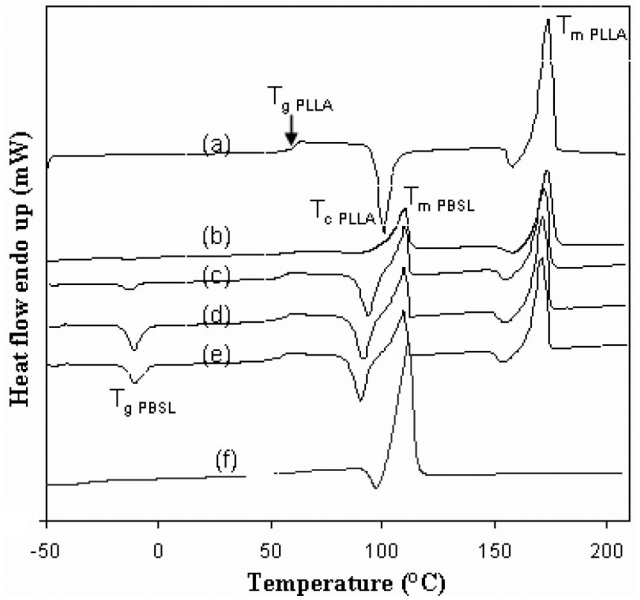

Figure 8. DSC thermograms of (a) virgin PLLA, (b) PASL, (c) PASL 0.5, (d) PASL 1, (e) PASL 2, and (f) PBSL.

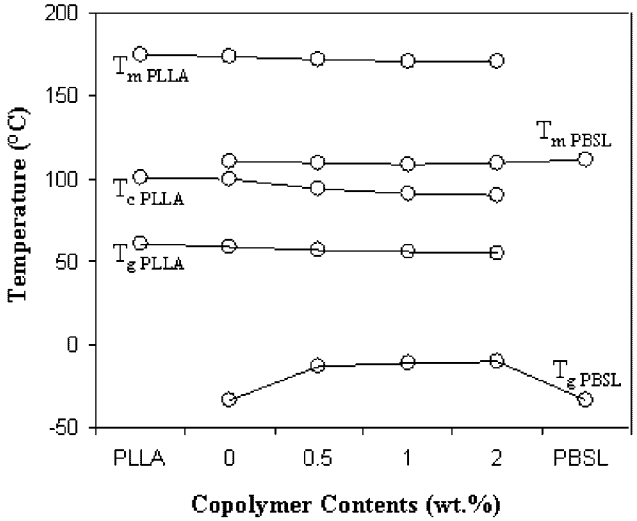

Figure 9. Phase diagram of virgin PLLA, PBSL, and the blends. (Note that 0 wt% of copolymer refers to PLLA/PBSL (PASL) blend).

in PLLA under certain crystallization conditions. According to a recent work,[27] this phenomenon can be explained by the possibility of recrystallization of lower perfection crystals of polylactide into α crystal of the higher perfection. In PLLA/PBSL blends (PASL), it is observed that overlapping of the T_c of PLLA and the T_m of PBSL occurred at about 100°C. The phase diagram in Fig. 9 also shows that the T_g, T_m, and T_c of PLLA decrease with an increase in the amount of copolymer. On the other hand, the T_g and T_m of PBSL increase with the increase in the proportion of copolymer. With the addition of triblock copolymer, the values of T_g of PLLA/PBSL blends get closer to each other at 22–27°C, compared with the values of the T_gs obtained from the PLLA/PBSL blends. The addition of copolymer reduces the gap of the T_g of both polymer blends; this indicates an improvement in the miscibility of the blends. In other words, this effect is considered to be a strong indication that complete segregation of PLLA and PBSL segments does not occur and that PLLA and PBSL are miscible, albeit partially. Furthermore, the T_ms of PLLA/PBSL blends slightly decrease and increase with the addition of copolymer, compared to their virgin polymers.

The level of crystallinity (X_c) of these virgin PLLA and the blends are shown in Table 4. It is apparent that the blend of PLLA/PBSL (PASL) showed the lowest crystallinity; this is because most of the X_c data for PLLA/PBSL cannot be measured owing to the overlapping phenomenon of T_c (PLLA) and T_m (PBSL) occurring in the blend system. Therefore, the data observed do not really represent the X_c of the PLLA. The PLLA/PBSL blend containing 2 wt% copolymer exhibits higher X_c value than that of PASL specimen and close to virgin PLLA value due to the addition of copolymer.

Figure 10 shows the FE-SEM micrographs of the cryo-fractured surfaces of the PLLA/PBSL blend, with and without the addition of the copolymer. In the case of PASL blend, a phase-separated system was observed where the PBSL phase exists in spherical shape dispersed in the continuous PLLA phase. The blend of immiscible polymers generally creates macro-phase separation of the two components owing to differences in solubility parameter.[23] Stress concentration usually takes place in the vicinity of the dispersed phase separations because of the differences in the elastic modulus

Table 4. The crystallinity of PLLA and the blends

Materials	ΔH_{cPLLA} (J/g)	ΔH_{mPLLA} (J/g)	X_{cPLLA} (%)
PLLA	30.0	56.1	91.5
PASL	2.4	28.0	46.7
PASL 2	18.2	40.1	89.6

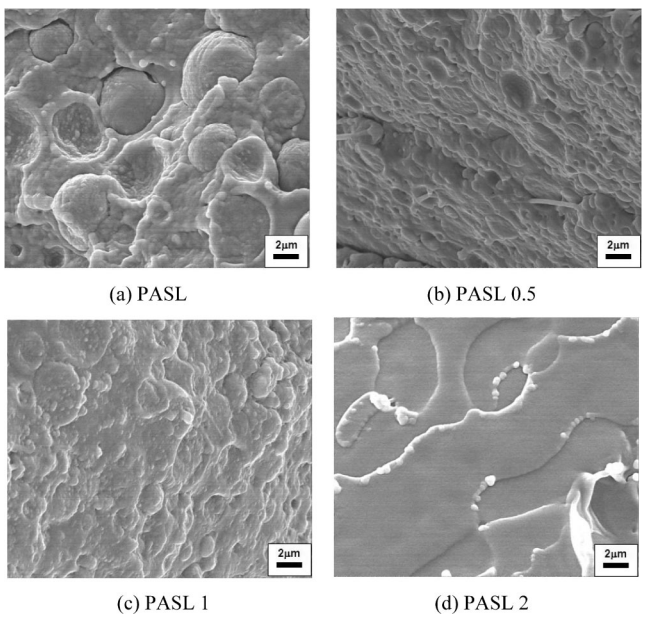

Figure 10. FE-SEM micrographs fractured surfaces under liquid nitrogen of PLLA/PBSL blends, with and without copolymer.

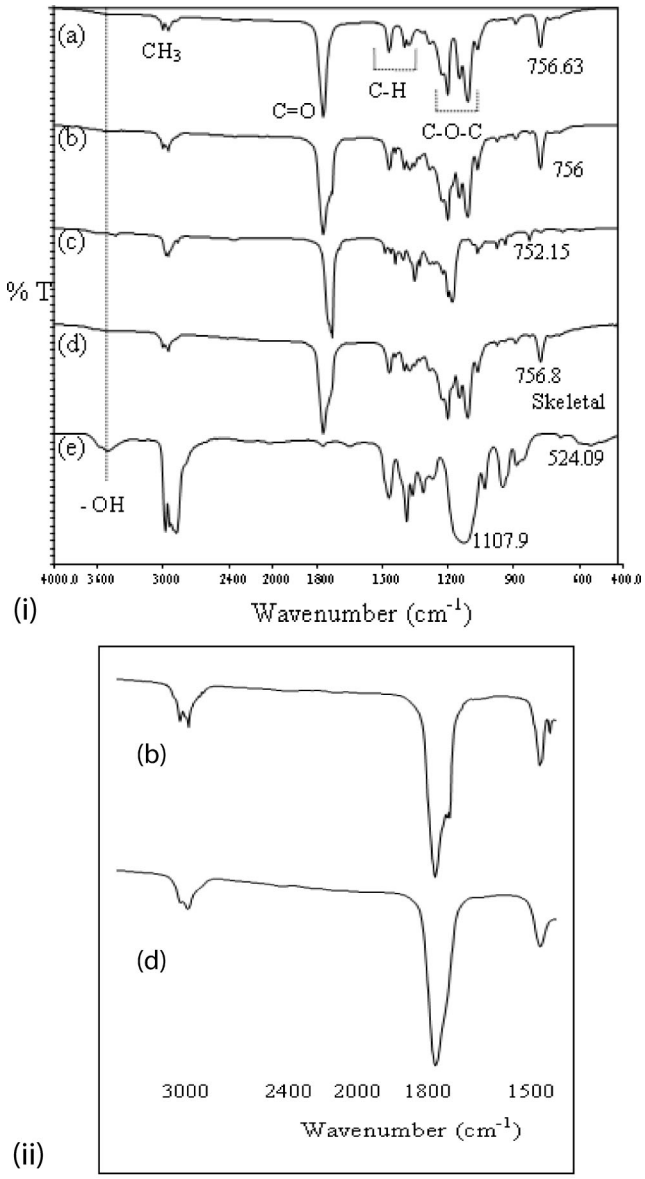

Figure 11. (i) FTIR spectra of (a) PLLA, (b) PASL, (c) PBSL, (d) PASL 2, (e) copolymer. (ii) Enlarged spectrum of (b) PASL and (d) PASL 2.

between the dispersed phases and the surrounding matrix, and initiates localized microdamages in this region. The phase separation subsequently affects the physical and mechanical properties of the blend.[1]

For comparison, the PLLA/PBSL blends with copolymer added are also shown in Figs. 10(b)–(d). The morphology of the phase-separated system, as shown in the PASL blend system, indicates that the number of spherical PBSL decreases dramatically resulting from the copolymer addition, and tends to further decrease with the increase in the copolymer content (as shown in the PASL 2 system).

FTIR spectroscopy analysis

Figure 11(i) shows the FTIR spectra of virgin PLLA and PBSL, copolymer, PLLA/PBSL blends with and without the addition of copolymer. The characteristic peak of the hydroxyl group (–OH) appears in the region 3440–3500 cm^{-1} for most of the spectra. As the end-group, their intensities consistently appeared quite weak due to their low molar content in the respective polymeric chains. Two distinct peaks in the regions 2850–2980 cm^{-1} correspond to the asymmetrical and symmetrical stretching mode of the CH_3 groups. Of note is the strong intensity for this peak in PEO-PPO-PEO copolymer consistently representing a higher molar content of the methyl group as compared to the polymer blends and virgin PLLA and PBSL. In all spectra, the C=O group occurred in the region 1751–1758 cm^{-1}, while that of C–O–C occurred in the region 1050–1200 cm^{-1}. Peaks in the region 1430–1480 cm^{-1} represent C–H deformation, while those at 733–756 cm^{-1} represent the skeletal vibration of the methylene groups.

The best way to analyze the FTIR data based on these propositions would be to compare the spectra of PASL and PASL 2 (refer to Fig. 11(ii)). Based on FTIR analysis, the peak in the region 1720 cm^{-1} which respond to C=O group appeared doubled for the sample without the addition PEO-PPO-PEO copolymer. This refers to the difference in bonding motion between that of PLLA and PBSL. However, after the addition of PEO-PPO-PEO copolymer, these peaks shift to a single broad peak, which indicate an identical bond motion in carbonyl group between the two copolymers. This can be attributed to the effect of the PEO-PPO-PEO copolymer, which formed good polar interaction between both PLLA and PBSL. This interaction

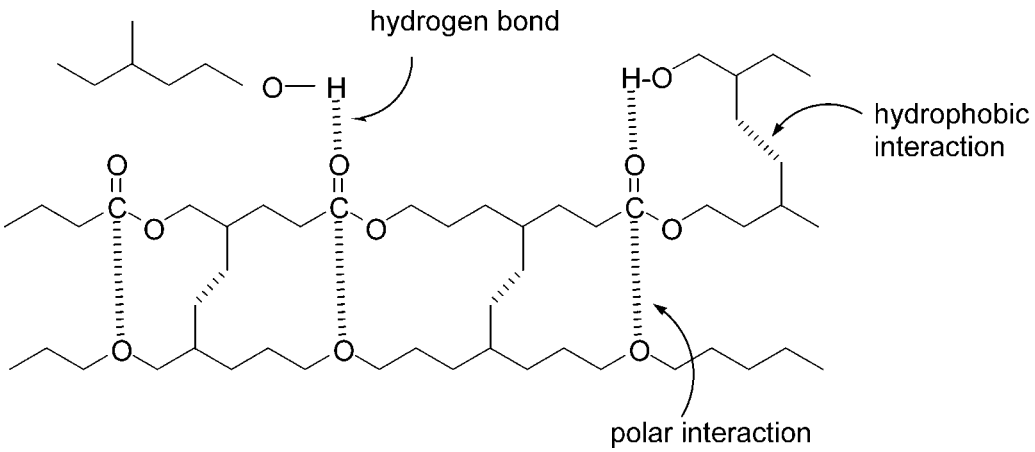

Figure 12. The possible physical interaction between the compatibilizer and the PASL matrix.

induces the mobilities of the respective carbonyl bonds as unit entity. This is in agreement with the previous works which showed changes in peak shift and intensity as the results of interchain of interaction due to the secondary process.[28,29] The overall possible physical interaction between the copolymer and the PLLA/PBSL blends is shown in Fig. 12.

CONCLUSIONS

The addition of PEO-PPO-PEO in PLLA/PBSL blends results in significant improvement in fracture toughness and bending properties of the PLLA/PBSL blend. However, insignificant thermal stability was observed in the PLLA/PBSL blends with the addition of copolymer. The complete segregation of PBSL phase in the PLLA continuous phase disappears with the addition of higher amount of the copolymer. It is proven by the morphological studies, where the number of spherical PBSL phase in PLLA dramatically decreases with the addition of copolymer. The miscibility increases as indicated in the DSC experiment, where the values of T_g in the PLLA/PBSL blends, with the addition of copolymer, get closer to each other at 22–27°C, compared with that of the PLLA/PBSL blend. This indicates that partial miscibility occurs in the blend system with the presence of copolymer and hence improves the mechanical properties of the blends. In general, the PEO-PPO-PEO triblock copolymer can be used to improve the toughness and compatibility of the PLLA/PBSL blends.

Acknowledgements

The authors would like to thank Toyota Motor Co., Ltd. and Mitsubishi Chemical Corporation for supplying the materials. The authors also greatly acknowledge the support of the Universiti Sains Malaysia and Kyushu University.

REFERENCES

[1] H. Tsuji, *Biomaterials* **2003**, *24*, 537–547.
[2] C.-G. Simon, Jr., N. Eidelman, S.-B. Kennedy, A. Sehgal, C.-A. Khatri, N.-R. Washburn, *Biomaterials* **2005**, *26*, 6906–6915.
[3] K.-S. Kim, I.-J. Chin, J. S. Yoon, H. J. Choi, D. C. Lee, K. H. Lee, *J. Appl. Polym. Sci.* **2001**, *82*, 3618–3626.
[4] E. E. Blumm, A. J. Owen, *Polymer* **1995**, *36*, 4077–4081.
[5] H. Tsuji, A. Mizuno, Y. Ikada, *J. Appl. Poly. Sci.* **1998**, *70*, 2259–2268.
[6] T. Takayama, M. Todo, *J. Mater. Sci.* **2006**, *41*, 4989–4992.
[7] T. Takayama, M. Todo, H. Tsuji, K. Arakawa, *J. Mater. Sci.* **2006**, *41*, 6501–6504.
[8] C.-C. Chen, J.-Y. Chueh, H. Tseng, H.-M. Huang, S.-Y. Lee, *Biomaterials* **2003**, *24*, 1167–1173.
[9] M. Shibata, Y. Inoue, M. Miyoshi, *Polymer* **2006**, *47*, 3557–3564.
[10] M. Harada, T. Ohya, K. Iida, H. Hayashi, K. Hirano, H. Fukuda, *J. Appl. Poly. Sci.* **2007**, *106*, 1813–1820.
[11] M. Todo, A. Harada, H. Tsuji, CD-ROM *Proceedings of the 16th International Conference on Composite Materials* **2007**, TuGM1-07
[12] M. Shibata, N. Teramoto, Y. Inoue, *Polymer* **2007**, *48*, 2768–2777.
[13] V. Vannaladsaysy, M. Todo, T. Takayama, M. Jaafar, Z. Ahmad, K. Pasomsouk, *J. Mater. Sci.* **2009**, *44*, 3006–3009.
[14] J. Lu, Z. Qiu, W. Yang, *Polymer* **2007**, *48*, 4196–4204.
[15] T. Takayama, M. Todo, *J. Mater. Sci.* **2006**, *41*, 4989–4992.
[16] V. Vilay, M. Mariatti, Z. Ahmad, M. Todo, K. Pasomsouk, *J. Appl. Polym. Sci.* **2009**, *114*(3), 1784–1792.
[17] H.-L. Chen, S.-F. Wang, *Polymer* **2000**, *41*, 5157–5164.
[18] Z. Qiu, T. Ikehara, T. Nishi, *Macromolecules* **2002**, *35*, 8251–8254.
[19] Z. Qiu, T. Ikehara, T. Nishi, *Polymer* **2003**, *44*, 3095–3099.
[20] T. Ikehara, H. Kurihara, Z. Qiu, T. Nishi, *Macromolecules* **2007**, *40*, 8726–8730.
[21] E. F. Lucas, R. S. Porter, *J. Appl. Polym. Sci.* **2003**, *49*, 1211–1222.
[22] C. M. Mahoney, *Anal. Chem.* **2005**, *77*, 3570–3578.
[23] M. Todo, S. D. Park, T. Takayama, K. Arakawa, *Eng. Fract. Mech.* **2007**, *74*, 1872–1883.
[24] H. Xu, C. Teng, M. Yu, *Polymer* **2006**, *47*, 3922–3928.
[25] H. Xu, M. Luo, M. Yu, C. Teng, S. Xie, *J. Macromol. Sci. Part B: Phy.* **2006**, *45*, 681–687.
[26] G. Maglio, A. Migliozzi, R. Palumbo, *Polymer* **2003**, *44*, 369–375.
[27] J. Zhang, Y. Duan, H. Sato, H. Tsuji, I. Noda, S. Yan, Y. Ozaki, *Macromolecules* **2005**, *38*, 8012–8021.
[28] J. Dong, Y. Ozaki, *Macromolecules* **1997**, *30*, 286–292.
[29] O. R. Pardini, J. I. Amalvy, *J. Appl. Polym. Sci.* **2008**, *107*, 1207–1214.

